Front. Phys. China, 2008, 3(3): 331–348
DOI 10.1007/s11467-008-0027-x

REVIEW ARTICLE

Jie ZHOU, Zong-hua LIU

Epidemic spreading in complex networks

Abstract The study of epidemic spreading in complex networks is currently a hot topic and a large body of results have been achieved. In this paper, we briefly review our contributions to this field, which includes the underlying mechanism of rumor propagation, the epidemic spreading in community networks, the influence of varying topology, and the influence of mobility of agents. Also, some future directions are pointed out.

Keywords network topology, epidemic spreading, rumor propagation, mobility, threshold

PACS numbers 87.19.Xx, 87.23.Ge, 89.75.Hc, 05.40.Fb

1 Introduction

The epidemic spreading in various complex networks has been quite extensively studied in recent years. One of the main reasons is that by using the network structure and modern transports/mediums, the epidemic can spread very fast and cause a series of problems to human society, such as an Internet virus, SARS (Severe Acute Respiratory Syndrome), and sexually transmitted diseases, etc. [1−3]. This topic has to do with the modeling of the spread of a particular infectious disease in a given network, with the aim of reproducing the actual dynamics of the disease and designing the strategies to control and possibly eradicate the infection. One of the primary reasons for studying the spread process on networks is to understand the mechanisms by which diseases and other things such as information, computer viruses, and rumors spread over these networks. In particular, most researches have been directed in two distinct directions. On the one hand, research has been focused on the configuration of networks, including the degree distribution, the clustering coefficient, and the assortativity etc., which reveals that simple dynamical rules, such as preferential attachment or selective rewiring, can generate complex topologies [1, 2, 4−13]. Many of these rules are not only useful for the generation of model graphs, but also believed to shape real-world networks like the Internet or the network of social contacts. On the other hand, attention has been paid to the dynamics in complex networks [14−22]. These studies have shown that the network topology can have a strong impact on the dynamics of the nodes, e.g., the availability of the percolation condition for networks with degree-degree correlation or the detrimental effect of assortative degree correlations on targeted vaccination. In the past, the cross fertilization between these two lines of thought has led to considerable advances. However, the network topology and the dynamics on networks are still generally studied separately and there is still a large enough space to combine them. One of the representative examples is how the epidemic is spread in complex networks.

Currently, researchers are try to model the epidemic spreading in complex networks and propose some effective approaches for potential applications. Mathematical models of viral transmission and control are always important tools for assessing the threat posed by deliberate release of the specific virus and the best means of containing an outbreak, such as the smallpox, measles, mumps, chickenpox, dengue haemorrhagic fever, pandemic influenza, tuberculosis, HIV, and foot-and-mouth disease, etc. [23−25]. Examples include the design and evaluation of childhood disease immunization programmes, predicting the demographic impact of

Jie ZHOU[1], Zong-hua LIU[1] (✉)

[1] Institute of Theoretical Physics and Department of Physics, East China Normal University, Shanghai 200062, China
E-mail: zhliu@phy.ecnu.edu.cn

Received March 9, 2008; accepted March 28, 2008

the HIV epidemic in different regions, and analysing the spread and control of the 2001 foot-and-mouth epidemic in Britain [26] etc.

In this paper, we will briefly review the recent achievements of epidemic spreading in complex networks and mainly focus on our contributions to this field. We will first address the basic models of epidemic spreading in Section 2. Then we address the epidemic spreading in general networks in Section 3. Next, we discuss how an epidemic is spread between two connected communities in Section 4. This problem has been recently addressed in the static community networks by Newman *et al.* [17, 27−29] and Liu *et al.* [30] where the community structures are fixed and the epidemic can be only spread from one community to another one through the links between them. After that, we study the mobile feature of social networks in Section 5. Finally, we give our conclusions and vision in Section 6.

2 Epidemic models

In complex networks, nodes represent the individuals and links represent the interactions between them. That is, there is a link between nodes if they have interaction; otherwise, there is no link. The infection can only be removed through the link between two nodes. The infection transmission is defined by the spreading rate at which each susceptible individual acquires the infection from an infected neighbor during one time step.

Suppose the infection rate is denoted by λ. One significant notion in the epidemic spreading is the location of the epidemic transition, i.e. a critical value of λ_c, such that for the infection rate $\lambda < \lambda_c$, no endemic epidemic is possible, while for $\lambda > \lambda_c$, a global epidemic spreading occurs with a finite probability [31, 32]. Thus, much attention has been paid to the study of the epidemic thresholds by different network structures [6, 7, 16, 17, 27−30, 33].

In reality, epidemic spreading is a very complicated process and its result depends on the concrete situations. For example, some diseases have immunization ability where a person cannot be infected again once he/she was infected one time, such as a computer virus and gonorrhea, etc. Other diseases have no immunization ability where a person can be infected again even if he/she was infected one time, such as parotitis, measles, and influenza, etc. Therefore, it is necessary to build different models to model them. In fact, a large number of models have been presented to describe different situations of epidemic spreading. Two of the typical models are the SIS model and the SIR model. As being close to real society, scale-free (SF) networks are the most popular networks in which disease spreading is studied. The absence of epidemic thresholds on scale-free networks has attracted lots of attention [33, 34].

2.1 SIS model

The SIS model relies on a coarse grained description of the individuals in the population. In the SIS model, the individuals may have two status, i.e., susceptible and infected. These states completely neglect the details of the infection mechanism within each individual. Once an individual is infected, he or she may become susceptible again after a finite time. Thus, this model describes the phenomenon that a susceptible node can become infected and an infected node can recover and return to the susceptible state [16, 30, 35−37], such as a computer virus, tuberculosis, and gonorrhea, etc. Suppose a neighbor of the infected node can be infected by probability λ and the infected node can be cured by probability μ. The SIS model can be described as follows:

$$\begin{aligned} &S(i) + I(j) \to I(i) + I(j) \\ &I(i) \to S(i) \end{aligned} \tag{1}$$

where the first equation occurs with rate λ and the second with rate μ, provided that i is one neighbor of j. When the susceptible and infected nodes are fully mixed, its dynamics can be described by the following differential equations:

$$\begin{aligned} \frac{\mathrm{d}s(t)}{\mathrm{d}t} &= -\lambda i(t)s(t) + \mu i(t) \\ \frac{\mathrm{d}i(t)}{\mathrm{d}t} &= \lambda i(t)s(t) - \mu i(t) \end{aligned} \tag{2}$$

where $s(t)$ and $i(t)$ represents the densities of susceptible and infected nodes at time t, respectively. There is a threshold λ_c in this model. The solution of Eq. (2) is $i(T) = 0$ for $\lambda < \lambda_c$ and a stationary solution for $\lambda > \lambda_c$. This model is mainly used as a paradigmatic model for the study of infectious disease that leads to an endemic state with a stationary and constant value for the prevalence of infected individuals, i.e., the degree to which the infection is widespread in the population.

2.2 SIR model

The second typical model is the three-state SIR (susceptible-infected-refractory) model which is well-known in mathematic epidemiology [31, 32]. This model describes the phenomenon that the infected nodes will become immunized or dead, such as parotitis, measles, chickenpox, pertussis, and influenza etc. [38−42]. Dif-

ferent from the case in the SIS model, here the infected nodes will not return to the susceptible status but become refractory status with probability μ. Once a node is in refractory status, it will no longer be susceptible to the infection. At a given time, each node in the network is in one of these three states. The SIR model is as follows:

$$\begin{aligned} &S(i)+I(j)\to I(i)+I(j)\\ &I(i)\to R(i) \end{aligned} \tag{3}$$

where the first equation occurs with rate λ and the second one with rate μ. When the susceptible and infected nodes are fully mixed, it allows writing down the SIR model in the form of systems of ordinary differential equations for the densities of individuals:

$$\begin{aligned} \frac{\mathrm{d}s(t)}{\mathrm{d}t}&=-\lambda i(t)s(t)\\ \frac{\mathrm{d}i(t)}{\mathrm{d}t}&=\lambda i(t)s(t)-\mu i(t)\\ \frac{\mathrm{d}r(t)}{\mathrm{d}t}&=\mu i(t) \end{aligned} \tag{4}$$

where $s(t)$, $i(t)$, and $r(t)$ are the densities of susceptible, infected, and refractory nodes at time t, respectively. As time goes on, obviously, this model will show an increasing number of infection nodes. At sufficiently large time, this number will begin to decrease until there is no longer any infected nodes in the network, then the process is over. Thus, there is a one-to-one correspondence between the final infected density $r(T)$ and the infection rate λ and the $r(T)$ can be used to measure the efficiency of infection, where T is the time when $i(t)$ becomes zero. There is also a threshold λ_{c} in this model. The infection will become endemic or global for $\lambda>\lambda_{\mathrm{c}}$ and cannot spread out for $\lambda<\lambda_{\mathrm{c}}$.

2.3 Other models

One of the differences between the SIS and SIR models is the different final state. In the SIS model, the final state is an oscillatory solution. While in the SIR model, the final state is the zero infected nodes in the network. Except these two typical models, there are other models, such as the SI, SIRS, and SEIR etc.

In the SI model, once the nodes are infected, they will be an infector forever [43−45]. This model usually describes the disease that cannot be cured or break out without any effective control at hand, such as bubonic plague and SARS, etc. The SI model is as follows:

$$S(i)+I(j)\to I(i)+I(j) \tag{5}$$

where the infection occurs with rate λ. Its dynamics can be described by the following differential equations:

$$\begin{aligned} \frac{\mathrm{d}s(t)}{\mathrm{d}t}&=-\lambda i(t)s(t)\\ \frac{\mathrm{d}i(t)}{\mathrm{d}t}&=\lambda i(t)s(t) \end{aligned} \tag{6}$$

In the SIRS model, the susceptible nodes can pass to the infected state through contagion by an infected one, the infected nodes can pass to the refractory state after an infection time τ_I, the refractory nodes can return to the susceptible state after a recovery time τ_R [14, 46]. SIRS models are excitable systems, known to display relaxation oscillations in mean field or well-mixed approaches.

In the SEIR model, there is a latent state E between the susceptible and infected status [47, 48]. A susceptible individual acquires the infection from any given infected individual, and becomes latent and then become infected. This set of states do not correspond strictly to any particular disease but encompasses the most relevant features and parameters of a variety of different virus transmission. The dynamical equations are as follows:

$$\begin{aligned} \frac{\mathrm{d}s(t)}{\mathrm{d}t}&=-w_{s\to e}e(t)s(t)\\ \frac{\mathrm{d}e(t)}{\mathrm{d}t}&=w_{s\to e}e(t)s(t)-w_{e\to i}e(t)\\ \frac{\mathrm{d}i(t)}{\mathrm{d}t}&=w_{e\to i}e(t)-w_{i\to r}i(t)\\ \frac{\mathrm{d}r(t)}{\mathrm{d}t}&=w_{i\to r}i(t) \end{aligned} \tag{7}$$

where $w_{s\to e}, w_{e\to i}, w_{i\to r}$ are the probabilities for a susceptible individual to become latent, a latent to become infected, and an infected to become refractory, respectively. The related situations are the seasonal influenza or SARS-like diseases [24, 25].

3 Epidemic spreading in general networks

In general, networks can be classified into homogeneous networks and heterogeneous ones, according to their degree distribution. Correspondingly, the epidemic spreading on them are different. For the former, the dynamics can be shown by the mean field or fully mixed approaches; While for the latter, the influence of degree distribution must be considered. A network is homogeneous provided its degrees are distributed around a mean value and its degree distribution decays exponentially, such as the Erdos and Renyi (ER) random network and the small-world network (SW) [1, 2]. Also, a network

is heterogeneous if its degree distribution satisfies the power law, such as the Barabasi and Albert SF network. In this section, we will briefly introduce the epidemic and rumor spreading on the homogeneous and heterogeneous networks, respectively, and show the surprising result of zero threshold in the SF network by Pastor-Satorras and Vespignani [35].

3.1 Epidemic spreading in homogeneous networks

Let us consider the SIS model first. At each time step, each susceptible node is infected with probability v if it is connected to one or more infected nodes. At the same time, infected nodes are cured and become susceptible again with probability μ, defining an effective spreading rate $\lambda = v/\mu$. Without loss of generality, we set $\mu = 1$ which changes only the evolution time scale. In standard topologies the most significant result is the general prediction of a nonzero epidemic threshold λ_c [31, 32]. If the value of λ is above the threshold $\lambda > \lambda_c$ the infection spreads and becomes persistent in time. Below it $\lambda < \lambda_c$, the infection dies out exponentially fast. We here use the mean-field approach to deal with the situation of homogeneous networks [49]. The density of infected node $\rho(t)$ satisfies the following differential equation:

$$\frac{\mathrm{d}\rho(t)}{\mathrm{d}t} = -\rho(t) + \lambda \langle k \rangle \rho(t)[1 - \rho(t)] \tag{8}$$

The first term on the right-hand side in Eq. (8) considers that infected nodes become healthy with unit rate. The second term represents the average density of newly infected nodes generated by each active node. This is proportional to the infection spreading rate λ, the number of links emanating from each node, and the probability that a given link points to a healthy node, $1 - \rho(t)$. Because the homogeneous network has only exponentially small fluctuations, we take $k \approx \langle k \rangle$ as the first approximation. Using the steady condition $\mathrm{d}\rho(t)/\mathrm{d}t = 0$, we obtain

$$\rho[-1 + \lambda \langle k \rangle (1 - \rho)] = 0 \tag{9}$$

for the steady state density ρ of infected nodes. This equation defines an epidemic threshold $\lambda_c = \langle k \rangle^{-1}$, and yields

$$\begin{aligned} &\rho = 0, \quad \text{if} \quad \lambda < \lambda_c \\ &\rho \sim \lambda - \lambda_c, \quad \text{if} \quad \lambda \geqslant \lambda_c \end{aligned} \tag{10}$$

For the SIR model, we use $s(t), i(t), r(t)$ to represent the densities of the susceptible, infected, and refractory nodes, respectively. These three quantities are linked through the conservative condition:

$$s(t) + i(t) + r(t) = 1 \tag{11}$$

and they obey the following differential equations [39]:

$$\begin{aligned} \frac{\mathrm{d}s(t)}{\mathrm{d}t} &= -\lambda \langle k \rangle i(t)s(t) \\ \frac{\mathrm{d}i(t)}{\mathrm{d}t} &= \lambda \langle k \rangle i(t)s(t) - i(t) \\ \frac{\mathrm{d}r(t)}{\mathrm{d}t} &= i(t) \end{aligned} \tag{12}$$

This set of equations is based on the homogeneous mixing hypothesis, which asserts that the force of infection is proportional to the density of infectious individuals. The homogeneous mixing hypothesis is indeed equivalent to a mean-field treatment of the model, in which one assumes that the rate of contacts between infectious and susceptible nodes is constant. Another implicit assumption of this model is that the time scale of the disease is much smaller than the lifespan of individuals; therefore we do not include in the equation terms accounting for the birth or natural death of individuals.

Different from the SIS model, here the infection is measured by the final infected population r_∞. When λ is below the threshold, $\lambda < \lambda_c$, the epidemic prevalence $r_\infty = \lim_{t\to\infty} r(t)$ is infinitesimally small in the limit of very large populations. If the value of λ is above λ_c, $\lambda > \lambda_c$, the disease spreads and infects a finite fraction of the population. Integrating Eq. (12) for $s(t)$ with the initial conditions $r(0) = 0$ and $s(0) \approx 1$ [i.e., assuming $i(0) \approx 0$], we obtain

$$s(t) = \mathrm{e}^{-\lambda \langle k \rangle r(t)} \tag{13}$$

Combining this result with the condition (11), we observe that the total number of infected individuals r_∞ fulfills the following self-consistent equation:

$$r_\infty = 1 - \mathrm{e}^{-\lambda \langle k \rangle r_\infty} \tag{14}$$

In order to have a nonzero solution, the following condition must be fulfilled:

$$\frac{\mathrm{d}}{\mathrm{d}r_\infty}(1 - \mathrm{e}^{-\lambda \langle k \rangle r_\infty})|_{r_\infty = 0} > 1 \tag{15}$$

This condition is equivalent to the constraint $\lambda > \lambda_c$, where the epidemic threshold λ_c takes the value $\lambda_c = \langle k \rangle^{-1}$ in this particular case. Performing a Taylor expansion at $\lambda = \lambda_c$ it is then possible to obtain the epidemic prevalence behavior:

$$r_\infty \sim (\lambda - \lambda_c) \tag{16}$$

3.2 Epidemic spreading in heterogeneous networks

In SF networks, because the degree distribution satisfies

the power-law, a random chosen node is prone to be connected to a hub node or a node with larger links. Thus, those nodes with larger links will be easily infected and then as seeds to infect other nodes, resulting in a faster epidemic spreading than the homogeneous networks. To characterize the influence of network topology, Pastor-Satorras and Vespignani classify the nodes into different groups where the nodes in the same group have the same degree/links [16, 35, 36, 39, 49]. For the SIS model, using ρ_k to represent the density of infected nodes in the group with degree k, then $\rho_k(t)$ satisfies the following differential equation:

$$\frac{\mathrm{d}\rho_k(t)}{\mathrm{d}t} = -\rho_k(t) + \lambda k[1-\rho_k(t)]\sum_{k'} P(k'|k)\rho_{k'}(t) \quad (17)$$

The first term on the right-hand side represents the annihilation of infected individuals due to recovery with unitary rate. The creation term is proportional to the density of susceptible individuals, $1-\rho_k$, times the spreading rate, λ, the number of neighboring nodes, k, and the probability that any neighboring node is infected. The latter is the average over all degrees of the probability $P(k'|k)\rho_{k'}$ that an edge emanated from a node with degree k points to an infected node with degree k'. This equation is somehow approximate because of the neglecting of higher-order density-density and degree correlations. Denoting $\sum_{k'} P(k'|k)\rho_{k'}(t)$ as $\Theta(\rho(t))$, Eq. (17) becomes

$$\frac{\mathrm{d}\rho_k(t)}{\mathrm{d}t} = -\rho_k(t) + \lambda k[1-\rho_k(t)]\Theta(\rho(t)) \quad (18)$$

In the steady (endemic) state, ρ is just a function of λ. Thus, the probability Θ becomes also an implicit function of the spreading rate, and by letting $\partial_t \rho_k(t) = 0$, we obtain

$$\rho_k = \frac{k\lambda\Theta(\lambda)}{1+k\lambda\Theta(\lambda)} \quad (19)$$

For an uncorrelated network, the probability $P(k'|k)$ equals $kP(k)/\langle k\rangle$, thus Θ can be also written as:

$$\Theta = \sum_{k'} P(k'|k)\rho_{k'} = \sum_k \frac{kP(k)}{\langle k\rangle}\frac{k\lambda\Theta(\lambda)}{1+k\lambda\Theta(\lambda)} \quad (20)$$

This is a self-consistency equation that allows to find $\Theta(\lambda)$ and an explicit form for Eq. (19). Finally, we can evaluate the order parameter ρ using the relation:

$$\rho = \sum_k P(k)\rho_k \quad (21)$$

The system (20) can be solved self-consistently obtaining that the epidemic threshold is given by [50]

$$\lambda_\mathrm{c} = \frac{\langle k\rangle}{\langle k^2\rangle} \quad (22)$$

For infinite SF networks with $P(k)\sim k^{-\gamma}$ and $\gamma \leqslant 3$, we have $\langle k^2\rangle = \infty$, and correspondingly $\lambda_\mathrm{c} = 0$. Therefore, the uncorrelated SF networks allow a finite prevalence whatever the spreading rate λ of the infection! This result explains why the virus/rumor can be spread so fast in the Internet or social networks.

For the SIR model, using the $s_k(t), i_k(t), r_k(t)$ to represent the densities of susceptible, infected, and refractory nodes in the group with degree k, these variables are connected by means of the normalization condition:

$$s_k(t) + i_k(t) + r_k(t) = 1 \quad (23)$$

Doing the similar analysis of the SIS case we obtain the following differential equations:

$$\begin{aligned}
\frac{\mathrm{d}s_k(t)}{\mathrm{d}t} &= -\lambda k s_k(t)\Theta(t)\\
\frac{\mathrm{d}i_k(t)}{\mathrm{d}t} &= -i_k(t) + \lambda k s_k(t)\Theta(t)\\
\frac{\mathrm{d}r_k(t)}{\mathrm{d}t} &= i_k(t)
\end{aligned} \quad (24)$$

Eq. (24) can be solved with the initial conditions $r_k(0) = 0, i_k(0) = i^0$, and $s_k(0) = 1 - i^0$. In the limit $i^0 \to 0$, we can substitute $i_k(0) \approx 0$ and $s_k(0) \approx 1$. Under this approximation, Eq. (24) can be directly integrated, yielding

$$s_k(t) = \mathrm{e}^{-\lambda k\phi(t)} \quad (25)$$

where $\phi(t)$ is an auxiliary function:

$$\phi(t) = \int_0^t \Theta(t')\mathrm{d}t' = \frac{1}{\langle k\rangle}\sum_k kP(k)r_k(t) \quad (26)$$

The variation of the auxiliary function can be given by its time derivative

$$\begin{aligned}
\frac{\mathrm{d}\phi(t)}{\mathrm{d}t} &= \frac{1}{\langle k\rangle}\sum_k kP(k)i_k(t)\\
&= \frac{1}{\langle k\rangle}\sum_k kP(k)(1-r_k(t)-s_k(t))\\
&= 1-\phi(t) - \frac{1}{\langle k\rangle}\sum_k kP(k)s_k(t)
\end{aligned} \quad (27)$$

Introducing the obtained time dependence of $s_k(t)$ we are led to the differential equation for $\phi(t)$

$$\frac{\mathrm{d}\phi(t)}{\mathrm{d}t} = 1-\phi(t) - \frac{1}{\langle k\rangle}\sum_k kP(k)\mathrm{e}^{-\lambda k\phi(t)} \quad (28)$$

Eq. (28) is a self-consistency equation and can be solved for a given $P(k)$. Once Eq. (28) is solved, we can obtain

the total epidemic prevalence r_∞ as a function of $\phi_\infty = \lim_{t\to\infty}\phi(t)$. Since $r_k(\infty) = 1 - s_k(\infty)$, we have

$$r_\infty = \sum_k P(k)(1 - \mathrm{e}^{-\lambda k\phi_\infty}) \tag{29}$$

We can also calculate the threshold λ_c here. Since we have that $i_k(\infty) = 0$ and consequently $\lim_{t\to\infty} \mathrm{d}\phi(t)/\mathrm{d}t = 0$, we obtain from Eq. (28) the following self-consistent equation for ϕ_∞:

$$\phi_\infty = 1 - \frac{1}{\langle k\rangle}\sum_k kP(k)\mathrm{e}^{-\lambda k\phi_\infty} \tag{30}$$

In order to have a non-zero solution, the condition

$$\frac{\mathrm{d}}{\mathrm{d}\phi_\infty}\left(1 - \frac{1}{\langle k\rangle}\sum_k kP(k)\mathrm{e}^{-\lambda k\phi_\infty}\right)\Big|_{\phi_\infty=0} > 1 \tag{31}$$

must be fulfilled. This relation implies

$$\frac{1}{\langle k\rangle}\sum_k kP(k)(\lambda k) = \lambda\frac{\langle k^2\rangle}{\langle k\rangle} > 1 \tag{32}$$

This condition defines the epidemic threshold:

$$\lambda_\mathrm{c} = \frac{\langle k\rangle}{\langle k^2\rangle} \tag{33}$$

which is the same with Eq. (22) of the SIS model.

3.3 Rumor spreading in complex networks

Rumor propagation can be considered as another kind of epidemic spreading which also follows the SIR model. Because of its characteristic feature, the explanation of its three states has a little difference [6, 7, 51−55]. Suppose there is a rumor or news in the network. The person (node) who has heard it and wishes to spread it is in the infected status, the one who has not heard it is in the susceptible status, and the one who has heard it but is no longer interested in spreading it is in the refractory status. The SIR model of Rumor is as follows:

$$\begin{aligned} &S(i) + I(j) \to I(i) + I(j)\\ &I(i) + I(j) \to R(i) + I(j)\\ &I(i) + R(j) \to R(i) + R(j) \end{aligned} \tag{34}$$

Rumor propagation was originally addressed by Sudbury [51] and recently investigated in networks by Zanette [52] and Liu *et al.* [6, 7, 55]. Sudbury's case is equivalent to rumor spreading on a complete random network, i.e., a homogeneous network. Sudbury finds that the rumor can only be propagated to 80 % population. Zanette studies the rumor propagation on small world networks by a mean-field approach and found that the percentage of nodes that have the chance to hear the rumor is less than 80 %. Liu *et al.* studied the case of a general network and found that the final percentage of the population who heard the rumor decreases with a network structure parameter p. We here follow the reference [55] to show how the network structure influence rumor propagation.

The idea can be explained with the help of Fig. 1. Consider two neighboring nodes A and B that are connected by a link in the network. Suppose node A is infected and transmits the rumor to node B at time t. Then at time $t+1$, node B will choose one of its neighbors as the target to transmit the rumor, which include node A. Because A is the "father" of B, A will not be at the same footing with the other neighbors of B. When A is chosen from the neighbors of B, B will become the refractory with the probability of unity according to the propagation rules. When one of the other neighbors of B, except A, is chosen, B becomes the refractory or remain as infected, depending on the status of the chosen node. That is, the probability for B to become refractory is less than unity. If the degree of B is k, the probability for choosing A is $1/k$ and the probability of choosing the others is $1 - 1/k$. Combining this analysis and the homogeneous mixing hypothesis, we obtain the evolution equations of $n_{k,S}$, $n_{k,I}$, $n_{k,R}$,

$$\begin{aligned} \dot{n}_{k,S} &= -\sum_{k'} n_{k',I}(t)\left(1 - \frac{1}{k'}\right)P(k'|k)\frac{n_{k,S}(t)}{N_k}\\ \dot{n}_{k,R} &= n_{k,I}(t)\left[\frac{1}{k} + \left(1 - \frac{1}{k}\right)\right.\\ &\quad\left.\cdot\sum_{k'} P(k'|k)\frac{n_{k',I}(t) + n_{k',R}(t)}{N_{k'}}\right] \end{aligned} \tag{35}$$

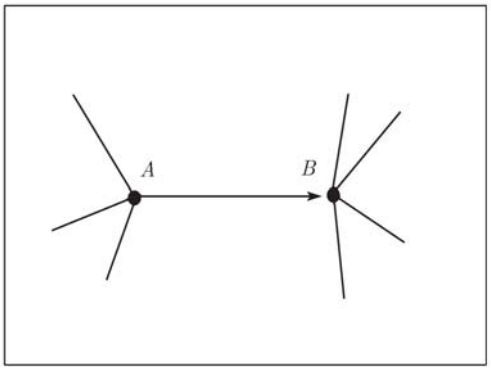

Fig. 1 Schematic illustration of the process of rumor transmitting: Suppose there is a link between node A and node B. At time t, node A gets the rumor and transmits it to node B. And then at time $t+1$, node B will transmit the rumor to one of its neighbors which includes node A. The key point is that the possibility for node B to become the refractory is unity when B chooses A as its target and less than unity when B chooses one of the other neighbors of B as its target.

where N_k denotes the number of nodes with the same degree k, $n_{k,S}(t)$, $n_{k,I}(t)$, $n_{k,R}(t)$ represent the numbers of the susceptible, infected, and refractory nodes with degree k at time t, respectively, the parts $n_{k,S}(t)/N_k$ and $[n_{k',I}(t)+n_{k',R}(t)]/N_{k'}$ come from the homogeneous mixing hypothesis. $n_{k,I}(t+1)$ can be obtained from the conservation condition $N_k = n_{k,S}(t) + n_{k,I}(t) + n_{k,R}(t)$.

We focus on the final density of the population that has the chance to hear the rumor. Let T be the time when the process of rumor spreading is over, i.e., $\sum_k n_{k,I}(T) = 0$. In obtaining the solution of Eq. (35) at time $t = T$, we introduce a set of auxiliary variables $s_k \equiv \int_0^T n_{k,I}(t)\mathrm{d}t$. Assume that the initial infected seed (at $t = 0$) has degree k_0, we have the initial conditions: $n_{k,S} = N_k$, $n_{k,I} = 0$, and $n_{k,R} = 0$ for $k \neq k_0$ and $n_{k,S} = N_k - 1$, $n_{k,I} = 1$, and $n_{k,R} = 0$ for $k = k_0$. We thus obtain the solutions of Eq. (35):

$$\begin{aligned} n_{k,S}(T) &= N_k \exp\left[\frac{-k}{\langle k\rangle N}\sum_{k'} s_{k'}\left(1-\frac{1}{k'}\right)\right] \\ n_{k,R}(T) &= N_k\left\{1-\exp\left[\frac{-k}{\langle k\rangle N}\sum_{k'} s_{k'}\left(1-\frac{1}{k'}\right)\right]\right\} \\ n_{k,I}(T) &= N_k - n_{k,S}(T) - n_{k,R}(T) = 0 \end{aligned} \tag{36}$$

By $n_{k,I}(T) = 0$ for different k, we may get a set of transcendental equations on s_k which can be accurately solved numerically. Hence, the final density of the refractory nodes with degree k is

$$\rho(k) \equiv \frac{n_{k,R}(T)}{N_k} = 1 - \mathrm{e}^{-\alpha k} \tag{37}$$

where $\alpha = \dfrac{1}{\langle k\rangle N}\sum_{k'} s_{k'}\left(1-\dfrac{1}{k'}\right)$ depends on the network structure. Obviously, $\rho(k)$ will monotonously increase with k and approaches to unity for large k. The total infected nodes during the spreading process is

$$N_R(T) \equiv \sum_k n_{k,R}(T) = N - \sum_k N_k \mathrm{e}^{-\alpha k} \tag{38}$$

The density of the total infected nodes is

$$\rho_R \equiv \frac{N_R(T)}{N} = 1 - \sum_k P(k)\mathrm{e}^{-\alpha k} = \sum P(k)\rho(k) \tag{39}$$

which depends on the degree distribution $P(k)$.

To confirm these predictions by numerical simulations, we construct a general network first. Take m nodes as the initial nodes and then add one node with m links at each time step. The m links from the added node will go to m existing nodes with probability $\Pi_i \sim (1-p)k_i + p$, where k_i is the degree of node i at that time and $0 \leqslant p \leqslant 1$ is a parameter. The resulting network has average degree $\langle k\rangle = 2m$ for large N. Obviously, $(1-p)k_i$ in Π_i represents the preferential attachment and p in Π_i the random attachment. According to Refs. [4, 5], for $p = 0$, the model generates a strictly scale-free network, while for $p = 1$, it generates a completely random network. For $0 < p < 1$, the resulting connectivity distribution is shown to be $P(k) \sim [k + p/(1-p)]^{-\gamma}$ [4, 5], where the scaling exponent γ is $\gamma = 3 + p/[m(1-p)]$.

First, we consider the case of scale-free network and let $N = 1000$, $m = 5$, and $p = 0$. We randomly choose a seed at $t = 0$ from which the infection starts. At each time step, every infected node contacts one of its neighbors, i.e., the nodes that are connected to it. If this node is susceptible, it will be infected; otherwise, the original infected node itself will lose interest in the rumor and become refractory. The whole process continues until time T at which there is no infected node. We count the refractory nodes with degree k, $n_{k,R}(T)$, and the total nodes with degree k, N_k, and then calculate the final density of infected nodes with degree k through $\rho(k) = n_{k,R}(T)/N_k$. We find that $\rho(k)$ increases monotonously with k when $k < 35$ and stay at $\rho(k) = 1$ or nearby when $k \geqslant 35$. The result is shown by "circles" in Fig. 2(a). Now we calculate the theoretical value of $\rho(k)$ through Eq. (37). The exponent α is obtained through its expression by calculating all the s_k at $t = T$ and then substituting α into Eq. (37) to get $\rho(k)$. "squares" in Fig. 2(a) shows how the theoretical $\rho(k)$ changes with k. Comparing the "circles" with the "squares" in Fig. 2(a) one can see that the theoretical results are consistent with the numerical experiments very well. We have found the similar results for the case of random network with $p = 1$. Figure 2(b) shows the re-

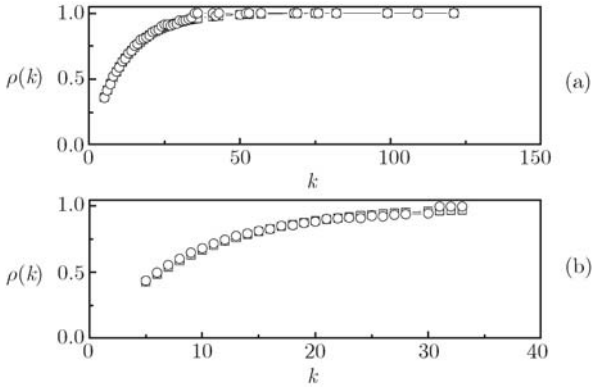

Fig. 2 $\rho(k)$ versus k. The results are obtained by 1000 realizations with $N = 1000$ and $\langle k\rangle = 10$. "circles" denote the numerical simulations and "squares" the theoretical predictions from Eq. (37), and **(a)** represents the case of scale-free network with $p = 0$ and **(b)** the case of random network with $p = 1$.

sults where the lines with "circles" denote the numerical simulations and the lines with "squares" the theoretical predictions.

Then we investigate how ρ_R varies with the structure parameter p. In numerical experiments, we produce different network structures for different p and randomly choose different seeds. Once the process of rumor spreading is over, we count the number $N_R(T)$ of the total final infected nodes for all the degree k and calculate the density ρ_R through $\rho_R = N_R(T)/N$. The result is shown in Fig. 3 by the "circles". For comparison, we also calculate the ρ_R through Eq. (39) (see "squares" in Fig. 3). Obviously, in Fig. 3 "squares" are very close to "circles". Furthermore, from Fig. 3 it is easy to see that ρ_R increases with the structure parameter p. This can be explained as follows: For the networks with the same average degree, scale-free network has more nodes with larger degree than that in the random network. Therefore, in scale-free networks with $p = 0$ the rumor can be easily transmitted to the hub nodes with the heaviest degree and then to the other nodes. Once the hub nodes are in the infected or refractory status, it will be easy for the other infected nodes to become refractory as they have larger probability to be connected to the hub nodes than to the other nodes. When the infected nodes choose the hub nodes as their targets of rumor spreading, they themselves become refractory. This feature disappears in the random network with $p = 1$, which results in a faster ending of rumor spreading in a scale-free network than in a random network.

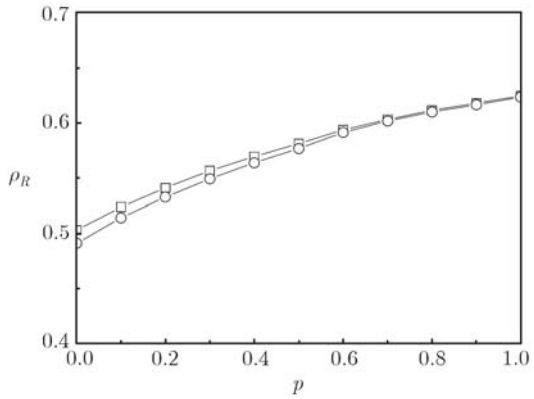

Fig. 3 ρ_R versus p. The results are obtained by using 1000 realizations with $N = 10^4$ and $\langle k \rangle = 10$. "circles" denote the numerical simulations and "squares" the theoretical predictions. The lines are drawn to guide the eye.

4 Epidemic spreading in community networks

A social network has a community structure [27−30]. The community may be classmates, friends, co-workers, and club members etc. In a social network, there are groups of nodes with many connections between their members and few connections to nodes outside the group, see the schematic Fig. 4. Thus, social networks have completely different structures with the above discussed general networks. Several approaches have been presented to construct the community networks [27−30, 56−60]. In this section, we follow the Ref. [30] to discuss how a community structure affects the infectious propagation.

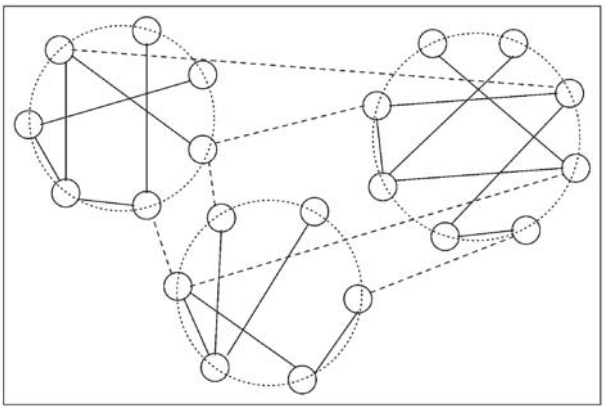

Fig. 4 Schematic illustration of the community network where the big dotted circles denote the groups, the small solid circles denote the nodes, the solid lines denote the links within the groups, and the dashed lines denote the links between groups.

4.1 Case of static community network

Considering that community structure has a high clustering coefficient and the links are dense in a community but sparse between communities, the community network can be constructed as follows [30]:

(1) Consider a network with N_0 nodes. Suppose the N_0 nodes are divided into m groups with random n_i ($i = 1, 2, \cdots, m$) nodes in each group, and let them satisfy $\sum_{i=1}^{m} n_i = N_0$.

(2) In each group i we use probability p to add a link between every two nodes, the resulting number of links are $\frac{1}{2}n_i(n_i - 1)p$.

(3) Between groups i and j we use probability q to add a link between every two nodes, the added links will be $n_i n_j q$.

Suppose the total number of added links is N, then we have $N = \sum_{i=1}^{m} \frac{1}{2}n_i(n_i - 1)p + \sum_{i<j}^{m} n_i n_j q$. Let $p/q \equiv \sigma$ be the degree of community, we get

$$p = \frac{N\sigma}{\sigma \sum_{i=1}^{m} \frac{1}{2} n_i(n_i-1) + \sum_{i<j}^{m} n_i n_j}$$
$$q = \frac{N}{\sigma \sum_{i=1}^{m} \frac{1}{2} n_i(n_i-1) + \sum_{i<j}^{m} n_i n_j} \quad (40)$$

It is a random network when $\sigma = 1$ and community network for $\sigma \gg 1$. For fixed N_0 and N, σ will determine the structure of the community network for a given set of n_i.

We use the SIS model to discuss the epidemic spreading on this model. Suppose the susceptible has a probability λ of contagion with each infected neighbor. If the node i is susceptible, and that it has k_i neighbors, of which $k_{\rm inf}$ are infected, then at each time step node i will become infected with probability $[1-(1-\lambda)^{k_{\rm inf}}]$. At the same time, each infected node will become susceptible at rate μ at each time step. To be brief, let us set $\mu = 1$, since it only affects the definition of the time scale of the virus propagation [31].

Suppose we have one seed in the beginning, then each neighbor of the seed will have possibility λ to be infected and then to infect their neighbors. After a finite time, the infection will reach a steady state which may be zero for $\lambda < \lambda_{\rm c}$ and nonzero for $\lambda > \lambda_{\rm c}$. Because of the heterogeneous structure of the community network, the final steady state will depend on the chosen seed and the configuration of the network. Thus, the meaningful result should be an average on different configurations and different initial conditions. This average is in fact a statistical average and can be obtained by a probability approach. From the theory of probability [60] we have $\lambda_{\rm c} = 1/\langle k_i \rangle$.

For a community network of $\sigma \gg 1$, when λ is small, the epidemic spreading will be confined within the group where the seed is chosen because the links between groups is much smaller than that within the group. Statistically, the seed will be chosen uniformly in each group. For a specific group i, its epidemic subthreshold $\lambda_{\rm c}^i$ will be determined by its average linking numbers. As the number of links between groups is much smaller than that within a group for $\sigma \gg 1$, we have $\lambda_{\rm c}^i \approx 1/\langle k_i \rangle \approx 1/p(n_i-1) \sim 1/p$ and this relation works for all the individual seed. The $\lambda_{\rm c}$ of the whole system is an average on different configurations and realizations, i.e., on different seeds, hence a qualitative relation between $\lambda_{\rm c}$ and p is $\lambda_{\rm c} \sim 1/p$. Substituting the expression of p in Eq. (40) into $\lambda_{\rm c}$ we have

$$\lambda_{\rm c} \sim \frac{1}{N}\left(1 + \frac{a}{\sigma}\right) \quad (41)$$

Thus, $\lambda_{\rm c}$ is inversely proportional to N. For a fixed N, Eq. (41) can be written as:

$$\lambda_{\rm c}(\sigma) - \lambda_{\rm c}(\infty) \sim \frac{1}{\sigma} \quad (42)$$

which is how $\lambda_{\rm c}$ depends on the degree of community when $\sigma \gg 1$.

To check the above analysis, let us make numerical experiments. We take $N_0 = 1000$, $N = 4 \times 10^4$, $m = 10$, and 100 configurations with different sets of random numbers $m_1(i), i = 1, 2, \cdots, m$. For each configuration, we take 100 different initial conditions with exactly one randomly chosen node infected. Thus we have 10^4 realizations. For each individual realization, the epidemic process will depend on its structure and the chosen seed. We find that, all the epidemic processes in the 10^4 realizations for small λ will die after a finite time, and only part of them will die for a relatively large λ, as shown in Fig. 5 for two typical processes where $n(t)$ is the infected number of individuals at time t. From both Fig. 5 (a) and (b) we can see that there are a lot of peaks corresponding to the disease quickly spreading through a community and then waiting to jump to the next one.

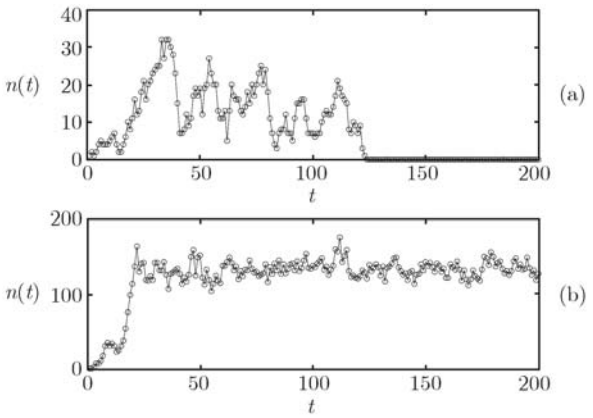

Fig. 5 Two typical processes of epidemic spreading for parameters $N_0 = 1000$, $N = 4 \times 10^4$, $m = 10$, and $\sigma = 100$ where **(a)** $\lambda = 0.008 < \lambda_{\rm c}$, **(b)** $\lambda = 0.015 > \lambda_{\rm c}$.

To check Eqs. (41) and (42), Fig. 6 shows the results of numerical simulations where (a) represents how $\lambda_{\rm c}$ depends on N for fixed σ and (b) how $\lambda_{\rm c}$ depends on σ for fixed N when $\sigma \gg 1$. The slopes of the two lines in Fig. 6(a) are unity, confirming $\lambda_{\rm c}$ linearly decrease with N for fixed σ in (41). In Fig. 6(b), the dashed line shows that the "circles" can be fitted into a straight line of slope unity when $\sigma > 200$, confirming Eq. (42) which is obtained under the condition $\sigma \gg 1$.

These results show that, with the decrease of the degree of community, the epidemic threshold of the community network will increase and reach its maximum at the limit of random network. For larger spreading rate,

it is easier for the epidemic on a random network to have global reach than that of a community network.

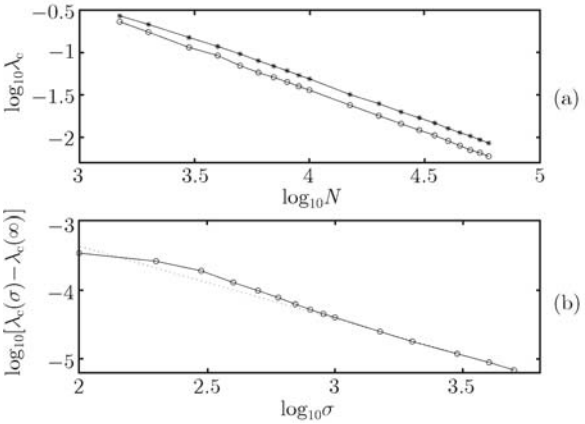

Fig. 6 Thresholds of epidemic spreading for the average of 10^4 realizations with $N_0 = 1000$ and $m = 10$. **(a)** λ_c versus N where the lines with "circles" and "stars" denote the cases of $\sigma = 100$ and 1, respectively. **(b)** λ_c versus σ for $N = 4 \times 10^4$.

4.2 One application of the community network model

In this subsection we use the above community network model as the underlying network structure to investigate the mechanism in spatiotemporal data of an epidemic in Thailand [61]. The dengue hemorrhagic fever (DHF) is a mosquito-borne virus that infects 50−100 million people each year. It has been reported that there is DHF in the 72 provinces of Thailand and the infection is a kind of periodic wave [24, 62]. The wave emanates from Bangkok, the largest city in Thailand, moving radially at a speed of 148 km per month to the outer provinces. These waves, which are superimposed on the basic yearly cycle, remain coherent up to 510 km from Bangkok. As a consequence the incidence data show strong seasonality and multiyear and intrayear oscillations and change in period over time.

We consider the SIS model and focus on its stationary state. In the stationary state, the links in one group are uniform and the infected nodes and the susceptible nodes are well-mixed. Hence, the evolution of infected nodes in a group can be reflected by the variation of the infected number $k_{\rm inf}$ of a node. We use $x(n)$ to denote $k_{\rm inf}$. Thus the variation of $x(n)$ will characterize the behaviors of the steady state. By the infection rate $[1-(1-\lambda)^{x(n)}]$ we know that the susceptible nodes will have a larger probability to be infected for larger $x(n)$. On the other hand, more $x(n)$ will result in less susceptible nodes, i.e., less candidates to be infected. Therefore, the iterated equation of $x(n)$ can be written as:

$$x(n+1) = [1-(1-\lambda)^{x(n)}][\langle k\rangle - x(n)] \tag{43}$$

where $\lambda_c < \lambda < 1$ and $\langle k\rangle - x(n)$ is the susceptible neighboring nodes of a node at time n. This discrete equation has a fixed point $\bar{x}$ which satisfies

$$\lambda = 1 - \left(\frac{\langle k\rangle - 2\bar{x}}{\langle k\rangle - \bar{x}}\right)^{1/\bar{x}} = 1 - f(\bar{x}) \tag{44}$$

From Eq. (44) we can easily get the derivative $\partial\lambda/\partial\bar{x}$ and find that $\partial\lambda/\partial\bar{x} = f(\bar{x})/\bar{x}^2 > 0$, indicating that λ increases with $\bar{x}$. When $\bar{x}$ approaches $\langle k\rangle/2$, $\partial\lambda/\partial\bar{x}$ will approach 0. To further increase λ, $\bar{x}$ will not be monotonous again but become period-2, i.e., one is larger than $\langle k\rangle/2$ and the other is smaller than $\langle k\rangle/2$. That is, there is a bifurcation point λ_b. The solution will jump between $\bar{x}_1$ and $\bar{x}_2$ when $\lambda > \lambda_b$:

$$\begin{aligned}\bar{x}_2 &= [1-(1-\lambda)^{\bar{x}_1}](\langle k\rangle - \bar{x}_1)\\ \bar{x}_1 &= [1-(1-\lambda)^{\bar{x}_2}](\langle k\rangle - \bar{x}_2)\end{aligned} \tag{45}$$

This is the epidemic spreading in a group. Considering the fact that the links between groups may also influence the epidemic spreading, the nodes in a group are not in the same position because some nodes have only the links in the group, while the others have both the links in the group and the links between the groups. This will result in the different infection rates for the neighbors of a node. As the differences change with time, let us treat it as a fluctuation of the infection rate. Considering that the influence/fluctuation from other groups will be stronger for the larger probability λ of contagion, Eq. (43) will be modified as

$$x(n+1) = [1-(1-\lambda)^{x(n)}][\langle k\rangle - x(n)] + D\lambda\xi(n) \tag{46}$$

where $\xi(n)$ is a uniform noise in $[0,1]$ and D is the noisy strength. Figure 7 shows the stabilized solution of Eq. (46). Obviously, it is period-1 for $0.015 < \lambda < 0.23$ and period-2 for $\lambda > 0.23$, and the period-1 approaches $\bar{x}(n) = \langle k\rangle/2 = 30$ when λ approaches to 0.23.

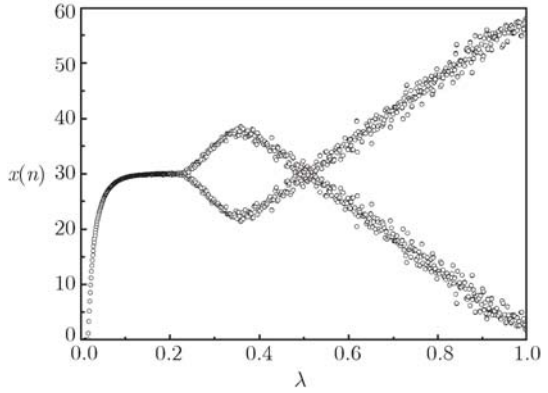

Fig. 7 In the stationary state, how the number of infected nodes depend on the infection rate from the analytic map (46), where $\langle k\rangle = 60$ and $D = 0.2$.

Now we use the SIRS model to reconsider this situation [61]. Our numerical simulation shows that the periodic waves are also possible in the SIRS model if we take a proper parameter τ_I and τ_R. A difference from the SIS model is that, there are two thresholds λ_{c1} and λ_{c2} for the SIRS model. The periodic waves exist only when $\lambda_{c1} < \lambda < \lambda_{c2}$ and disappear when out of this range. The reason for λ_{c1} is the same as in the SIS model. The reason for λ_{c2} is that the existence of the interval τ_I makes more people become infected and hence it is possible for all of them to become refractory during the time interval τ_R. Once it happens, the epidemic spreading will be ended. Figure 8 shows a typical pattern of periodic wave when λ is in between the range $[\lambda_{c1}, \lambda_{c2}]$ where (a) represents the change of the infected locations with time and (b) shows how the infected number changes with time. Combined with the results obtained in the SIS model, we see that the epidemic spreading in the community network has illustrated the spatio-temporal wave and may shed light on the understanding of the mechanism of DHF.

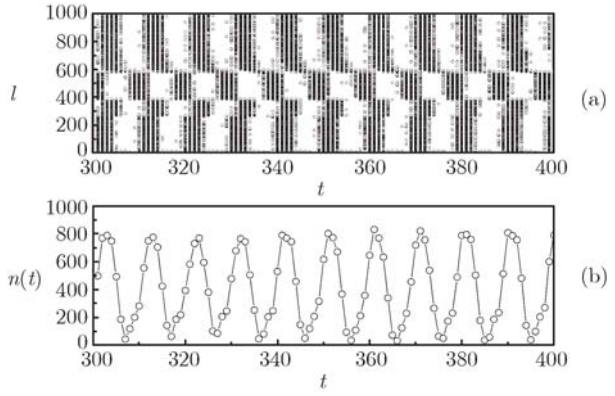

Fig. 8 Evolution of infection in SIRS model with $N_0 = 1000$, $N = 40\ 000$, $m = 10$ and $\sigma = 100$ where **(a)** represents the infected locations versus t and **(b)** the final infected number $n(t)$ versus t for $\tau_I = 4, \tau_R = 4$ and $\lambda = 0.12$.

4.3 Case of adjustable community network

The two most important quantities to characterize the structure of complex networks are the degree distribution and clustering coefficient. In this section, we discuss how the changing of degree distribution and clustering coefficient in a community network influences the epidemic spreading.

Observing the fact that a new friendship is formed between two people through an introducer of a common old friend in a community activity, the clustering of friends in a community can be modelled by a triad formation approach [56] in which a link is put between two neighbors of one node. This approach also fit for the links between different groups. Considering the fact that a friendship may also come from introducing oneself, the preferential attachment principle should also be taken. Based on these aspects, Wu and Liu recently presented a social network model with multiple community structure as follows [60]:

(1) Initially, there are m_0 groups. In each group, there are m_1 nodes which are completely connected to each other. In this paper, we let $m_0 = m_1 = 3$.

(2) At every time step, each group is added a new node with probability p, i.e., the total added nodes are $m_0 p$. Each added new node will emit m links to the existing nodes of the same group. Here we choose $m = 2$. The first link will be preferentially attached to a node-i with probability $k_i / \sum k_j$ where k_i represents the links of node-i and j in the sum is for all the nodes in the group. The second link will be randomly connected to one of the neighbors of node-i with probability q and be preferentially connected to anyone in the group with probability $1 - q$. Therefore, the evolution of k_i can be given by

$$\frac{\partial k_i}{\partial t} = p\left[\frac{k_i}{\sum\limits_j k_j} + qk_i\left(\frac{k_n}{\sum\limits_j k_j}\frac{1}{k_n}\right) + (1-q)\frac{k_i}{\sum\limits_j k_j}\right] = 2p\frac{k_i}{\sum\limits_j k_j} \tag{47}$$

where the term $k_i\left(\frac{k_n}{\sum_j k_j}\cdot\frac{1}{k_n}\right)$ comes from the k_i neighbors of node-i.

(3) At each time step, we preferentially choose a node-i in each group with probability $1 - p$ and let it emit m links to m nodes in other groups, i.e., the total added links are $mm_0(1-p)$. The m nodes can be chosen as follows: we first choose one group randomly from the other two groups. Then we preferentially choose a node from the chosen group for the first link, and the second link will randomly go to one neighbor of the chosen node with probability q and preferentially go to anyone in the chosen group with probability $1 - q$. Their contribution to the evolution of k_i is

$$\frac{\partial k_i}{\partial t} = (1-p)\left[2\frac{k_i}{\sum\limits_j k_j} + \frac{k_i}{\sum\limits_j k_j} + qk_i\left(\frac{k_n}{\sum\limits_j k_j}\frac{1}{k_n}\right) + (1-q)\frac{k_i}{\sum\limits_j k_j}\right]$$

$$= 4(1-p)\frac{k_i}{\sum_j k_j} \tag{48}$$

where the term $\frac{k_i}{\sum_j k_j} + qk_i\left(\frac{k_n}{\sum_j k_j}\frac{1}{k_n}\right) + (1-q)\frac{k_i}{\sum_j k_j}$ comes from the other two groups.

(4) Repeat the steps (2) and (3) until the nodes in each group is N_0. That is, the total nodes in the network is $N = m_0 N_0$ and the evolution will be stopped when $t = (N_0 - m_0)/p$.

By adding Eqs. (47) and (48) we obtain

$$\frac{\partial k_i}{\partial t} = 2(2-p)\frac{k_i}{\sum_j k_j} \tag{49}$$

When t is large, we have $\sum_j k_j = m_1(m_1-1) + 2mt \approx 2mt$. For a node added at time t_i, its initial condition is $k_i(t_i) = m = 2$. Substituting these into Eq. (49) we obtain the solution

$$k_i(t) = 2\left(\frac{t}{t_i}\right)^{\frac{2-p}{m}} \tag{50}$$

The probability of a node with degree $k_i(t) < k$ can be written as

$$\begin{aligned} P[k_i(t) < k] &= P\left[t_i > \left(\frac{2}{k}\right)^{\frac{m}{2-p}} t\right] \\ &= 1 - \left(\frac{2}{k}\right)^{\frac{m}{2-p}} \frac{t}{t+m_0} \end{aligned} \tag{51}$$

Thus, we have

$$P(k) = \frac{\partial P[k_i(t) < k]}{\partial k} = 2^{\frac{m}{2-p}} \frac{m}{2-p} k^{-\frac{m}{2-p}-1} \tag{52}$$

Obviously, it is a power-law degree distribution.

Another important quantity to characterize the network structure is the clustering coefficient, C, which characterizes the possibility for one's friends to become friends with each other. For a node-i with degree k_i, its clustering coefficient $C_i = \frac{2E_i}{k_i(k_i-1)}$ where E_i represents the total links among the k_i neighbors of node-i. The clustering coefficient of the network equals the average of all the C_i, i.e., $C = \frac{1}{N}\sum C_i$. From the algorithm (1) to (4) we know that E_i is proportional to q. Thus, we have

$$C \sim q \tag{53}$$

In sum, p controls the degree distribution and q controls the clustering coefficient. Therefore, both $P(k)$ and C can be continually changed through p and q. A key feature of this model is that the degree distribution $P(k)$ in Eq. (52) is independent of the parameter q! Therefore, we can keep the $P(k)$ unchanged and study the influence of C on the epidemic spreading through adjusting q.

We consider the SIR model here. For a tree-like network with the same degree k at every node, an infected node will make k infected nodes in the first step and $k(k-1)$ infected nodes in the second step. However, for a clustered network with the same degree k and a clustering coefficient C, an infected node will make k infected nodes in the first step and $k(k-1-2E/k) = k(k-1)(1-C)$ infected nodes in the second step where E is the links among the neighbors of a node. When $C = 1$, the epidemic spreading will stop at $t = 1$. Therefore, the epidemic spreading is linearly reduced by a factor $1 - C$. Returning to our model, we use $f(C)$ to characterize the influence of high clustering on the speed of epidemic spreading, where $f(C)$ satisfies $0 < f(C) < 1$ and $\mathrm{d}f(C)/\mathrm{d}C < 0$. Based on these analyses, we have

$$\begin{aligned} \frac{\mathrm{d}s_k(t)}{\mathrm{d}t} &= -\lambda k s_k(t) f(C) \sum_{k'} \frac{k' P(k') i_{k'}(t)}{\langle k \rangle} \\ \frac{\mathrm{d}i_k(t)}{\mathrm{d}t} &= -i_k(t) + \lambda k s_k(t) f(C) \sum_{k'} \frac{k' P(k') i_{k'}(t)}{\langle k \rangle} \\ \frac{\mathrm{d}r_k(t)}{\mathrm{d}t} &= i_k(t) \end{aligned} \tag{54}$$

where the mean-field approach is used, and the sum $\sum_{k'} k' P(k') i_{k'}(t) / \langle k \rangle$ is the probability that a randomly chosen link points to an infected node. Suppose, in the beginning, every node has the same possibility to be infected. Hence the initial condition is $r_k(0) = 0$, $i_k(0) = 1/NP(k)$, and $s_k(0) = 1 - i_k(0)$. In the limit $i_k(0) \to 0$, $s_k(0) \approx 1$. Integrating the first equation of Eq. (54) we obtain

$$s_k(t) = \mathrm{e}^{-\lambda k f(C) \phi(t)} \tag{55}$$

where the auxiliary variable $\phi(t)$ is defined as:

$$\phi(t) = \int_0^t \sum_{k'} \frac{k' P(k') i_{k'}(t')}{\langle k \rangle} \mathrm{d}t' = \frac{\sum k' P(k') r_{k'}(t)}{\langle k \rangle} \tag{56}$$

The derivative of $\phi(t)$ can be expressed as:

$$\frac{\mathrm{d}\phi(t)}{\mathrm{d}t} = \frac{\sum k' P(k')(1 - s_{k'}(t) - r_{k'}(t))}{\langle k \rangle}$$

$$= 1 - \phi(t) - \frac{\sum k' P(k') \mathrm{e}^{-\lambda k' f(C)\phi(t)}}{\langle k \rangle} \tag{57}$$

At the end of the infection process, we have $t = \tau$ and $\mathrm{d}\phi(t)/\mathrm{d}t = 0$, yielding

$$\phi(\tau) = 1 - \frac{\sum k' P(k') \mathrm{e}^{-\lambda k' f(C)\phi(\tau)}}{\langle k \rangle} \tag{58}$$

The total epidemic prevalence is

$$R \equiv \sum P(k) r_k(\tau) = 1 - \sum P(k) \mathrm{e}^{-\lambda k f(C)\phi(\tau)} \tag{59}$$

From Eq. (52) one can obtain that $\mathrm{d}P(k)/\mathrm{d}p > 0$ for $k < 5$ and $\mathrm{d}P(k)/\mathrm{d}p < 0$ for $k > 5$. Combining this result with the exponential decay of $\mathrm{e}^{-\lambda k f(C)\phi(\tau)}$ with k, we have the result that the second term in Eq. (59) increases with p, which gives

$$\frac{\mathrm{d}R}{\mathrm{d}p} < 0 \tag{60}$$

Recalling that $C \sim q$ in Eq. (53), then from Eq. (59) one can easily get that

$$\frac{\mathrm{d}R}{\mathrm{d}q} < 0 \tag{61}$$

Hence, the prevalence R is a monotonous decreasing function of both p and q.

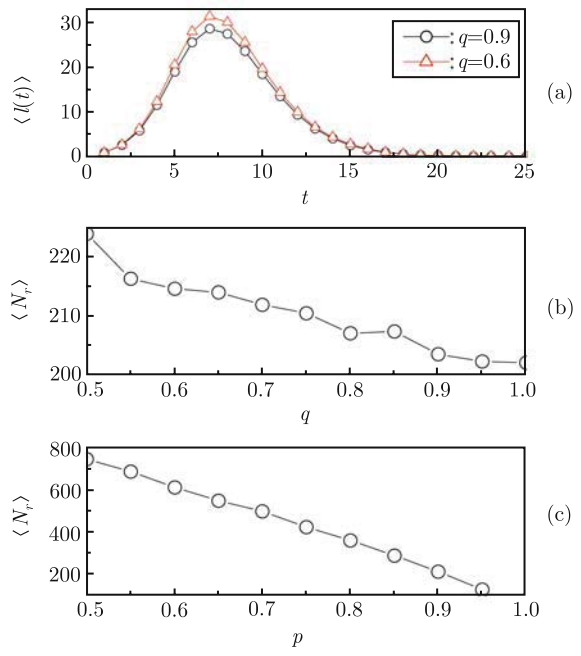

Fig. 9 How the structure parameters p and q influence the epidemic prevalence for $N = 3000$ and $\lambda = 0.2$. **(a)** $\langle I(t) \rangle$ versus t for $p = 0.9$ where the "circles" and "triangles" represent the cases of $q = 0.9$ and 0.6, respectively; **(b)** $\langle N_r \rangle$ versus q for $p = 0.9$; and (c) $\langle N_r \rangle$ versus p for $q = 0.9$. The results are averaged on 10^4 realizations.

To confirm the predictions (60) and (61), let us make numerical simulations. Figure 9 (a) shows how the number of infected nodes $I(t)$ changes with time for different q. The integration of $I(t)$ is the final infected nodes N_r in a realization. As $\langle N_r \rangle = NR$, we here use $\langle N_r \rangle$ to replace R to check Eqs. (60) and (61). Figure 9 (b) and (c) show how $\langle N_r \rangle$ changes with q and p, respectively. Obviously, $\langle N_r \rangle$ decreases with both p and q, confirming the theoretic predictions (60) and (61). Moreover, comparing Fig. 9(b) with (c) we can see that p has a larger influence on $\langle N_r \rangle$ than q, indicating that the efficiency of epidemic spreading depends mainly on the degree of community.

5 Epidemic spreading in dynamical networks

Through the above discussion, we may come to the conclusion that the epidemic behavior is determined by both the epidemic dynamics and the network's structure. Based on this conclusion, a number of methods have been proposed to immunize or control the epidemic spreading in complex networks [64−67]. It is generally believed that a community is safe if its connections to the surrounding infected communities are removed [64, 67]. However, the real situations are very complex. On one hand, there is a time delay between the infection of an agent and the knowledge of its status by others, which causes some difficulty to timely figure out the dangerous connections. On the other hand, the epidemic spreading may go through a third one, i.e., a community between a safe community and an infected one. However, to sustain the normal function of a community, we cannot remove all its connections to the surroundings, i.e., the connections to its safe surroundings should remain. Thus, if one of our neighboring community contacts with an infected community, how is our community influenced through the neighboring community?

Consider the fact that an agent can freely move in a community, with its neighbors changing with time [68−72]. Hence, we may conceive a dynamical network that is more close to a real society. Suppose an agent interacts only with its neighbors within radius r, i.e., there are links between those agents whose distance is smaller than r. Thus, the links are time dependent and the degree k of an agent depends on how many agents are within the circle of radius r. Each node in one community moves as follows:

$$\boldsymbol{x}_i(t + \Delta t) = \boldsymbol{x}_i(t) + \boldsymbol{v}_i(t)\Delta t \tag{62}$$

where $\boldsymbol{x}_i(t)$ is the position of the ith agent in the plane at time t, $\boldsymbol{v}_i(t) = (v\cos\,\theta_i(t), v\sin\,\theta_i(t))$, $\theta_i(t) = \xi_i(t)$, $\xi_i(t)$

are N independent random variables chosen at each time with uniform probability in the interval $[-\pi, \pi]$, and the velocity amplitude v is chosen as 0.03.

Also noticing that agents may sometimes travel to other communities, we let each agent have a possibility p to jump to a neighboring community. That is, each agent is a random walker with a probability p to travel to another community and the probability $1-p$ to stay in the community. Figure 10 shows the schematic network of two communities where each one is a square-shaped area with periodic boundary condition. In contrast to the real world, these areas could represent different cities that have a long geographical distance between them. People can move freely in his own city and travel to other cities by transports, such as an airplane, etc. We here follow the Ref. [73] to discuss its epidemic propagation.

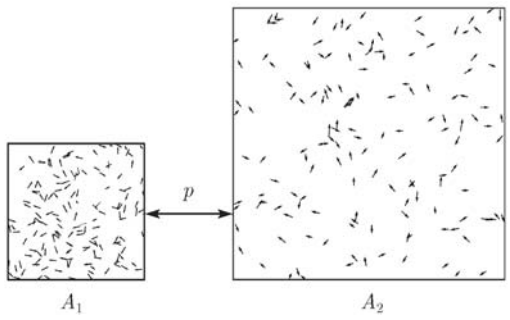

Fig. 10 Schematic illustration of epidemic spreading in the dynamical community network where the small segments with arrow denote the moving individuals and the bridge between the two communities represents the jumping of agents.

The SIS model is considered here. We let the length of A_1 be L_1 and the length of A_2 be L_2, we have the threshold $\lambda_{c1} \sim L_1^2/(\pi r^2 N)$ and $\lambda_{c2} \sim L_2^2/(\pi r^2 N)$. Without the jumping between A_1 and A_2 ($p = 0$), our numerical simulations have confirmed the λ_c phenomenon that the infection will continue when $\lambda > \lambda_c$ but die when $\lambda < \lambda_c$. Using $I(t)$ to denote the number of infected nodes at time t, $I(t)$ will become stabilized after a finite time, which is zero for $\lambda < \lambda_c$ and nonzero for $\lambda \geqslant \lambda_c$. We fix $N = 1000$, $r = 0.05$, $L_1 = 0.5$ and $L_2 = 1$ if without specific illustration. Hence, $\lambda_{c1} = 0.034 < \lambda_{c2} = 0.125$. For convenience, we call the community with $\lambda > \lambda_c$ as an infected community and the community with $\lambda < \lambda_c$ as a safe community.

When $p > 0$, the situation will be totally changed. Because of the jumping, it is even possible for the case of $\lambda < \lambda_c$ to sustain an epidemic. Taking λ in the regime $\lambda_{c1} < \lambda < \lambda_{c2}$, A_1 is the infected community and A_2 is the safe community. We want to know if the jumping can sustain a non-zero epidemic in the safe community A_2.

We use I_1 and I_2 to represent the numbers of infected agents in A_1 and A_2, respectively. Considering that each agent in A_1 has the possibility p to jump to A_2 and the agent in A_2 also has the possibility p to jump to A_1, the total infected number just before the time step $t+1$ is

$$\begin{aligned} I_1'(t) &= I_1(t)(1-p) + I_2(t)p \\ I_2'(t) &= I_2(t)(1-p) + I_1(t)p \end{aligned} \tag{63}$$

Therefore, the infected number at the beginning of time step $t+1$ is

$$\begin{aligned} I_1(t+1) &= [N - I_1'(t)][1 - (1-\lambda)^{\langle k\rangle_1 I_1'(t)/N}] \\ I_2(t+1) &= [N - I_2'(t)][1 - (1-\lambda)^{\langle k\rangle_2 I_2'(t)/N}] \end{aligned} \tag{64}$$

where $\langle k\rangle_1$ and $\langle k\rangle_2$ denote the average degrees in A_1 and A_2, respectively. Eqs. (63) and (64) are based on a mean-field approximation, their correctness can be checked on statistical meaning. For a given $\lambda_{c1} < \lambda < \lambda_{c2}$ and initial nonzero $I_1(0)$ and $I_2(0)$, Eq. (64) will go to a fixed point solution I_1^* and I_2^* after the transient process. Of course, this solution depends on the jumping probability p. By letting $I_2^*(t+1) = I_2^*(t)$, we have

$$I_2^* = [N - I_1^* p - I_2^*(1-p)]\{1 - (1-\lambda)^{\langle k\rangle_2 [I_2^*(1-p) + I_1^* p]/N}\} \tag{65}$$

For small p, we have $I_2^*/N \ll 1$. Approximately treating the first part of Eq. (65) as N and expanding its second part to the first order, we obtain

$$I_2^* = \frac{\lambda \langle k\rangle_2 I_1^* p}{1 - \lambda \langle k\rangle_2 (1-p)} \tag{66}$$

It is easy to see that I_2^* increases monotonously with p. This prediction has been well confirmed by numerical experiments. In numerical simulations, we determine I_1^* and I_2^* by checking the evolution of $I_1(t)$ and $I_2(t)$ and taking their stabilized values, and then making average

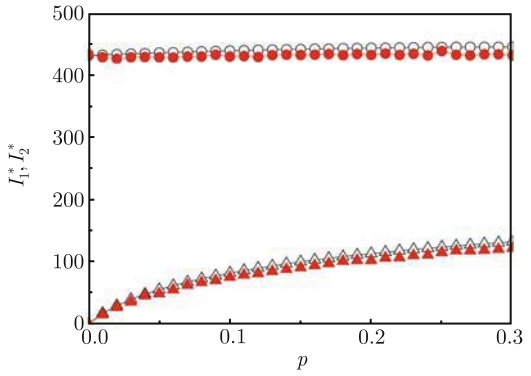

Fig. 11 Stabilized solution I_1^* and I_2^* versus the jumping probability p where the solid points represent the results of numerical simulations and the hollow points the results from Eq. (64), and the "circles" represent I_1^* and the "triangles" I_2^*. The results of numerical simulations are averaged on 100 realizations.

on a number of realizations. For example, Fig. 11 shows the results for $\lambda = 0.1$ where the solid points represent the results of numerical simulations and the hollow points the results from Eq. (64). Obviously, the numerical simulations are very well consistent with the theoretical predictions.

Why can the jumping agents make the safe community A_2 sustain the epidemic? To understand its mechanism, let us analyze the function of jumping agents in detail. Without jumping agents, the initial seeds in A_2 will die after the transient time. While with jumping agents, after the transient time, the infected agents $I_2(t+1)$ comes partly from the jumping part $I_1(t)p$ and partly from the remaining part $I_2(t)(1-p)$ which is also determined by the previous jumping parts. That is, the stabilized I_2^* comes completely from the jumping. Therefore, it is necessary to introduce a parameter γ to represent the efficiency of the jumping agents in A_2 to re-produce infectors. Notice that the slope of I_2^* in Fig. 11 decreases with p, indicating that I_2^* does not increase linearly with p. This point can be also seen from Eq. (66) where the slope

$$\frac{\mathrm{d}I_2^*}{\mathrm{d}p} = \frac{\lambda \langle k \rangle_2 I_1^*}{1 - \lambda \langle k \rangle_2 (1-p)} \left(1 - \frac{I_2^*}{I_1^*}\right) \tag{67}$$

decreases with p, indicating the influence of p in the denominator of Eq. (66) makes the slope decrease. Thus, the efficiency γ depends on p and can be given by the following formula:

$$\gamma = I_2^* - pI_1^* \tag{68}$$

which reflects the reproducing ability of the jumping agents. We find that there is an optimal p_0, γ increases with p when $p < p_0$ and decreases with p when $p > p_0$. Figure 12 shows the result for $\lambda = 0.1$ and $p_0 \approx 0.1$. The decrease of γ for $p > p_0$ comes from the fact that larger

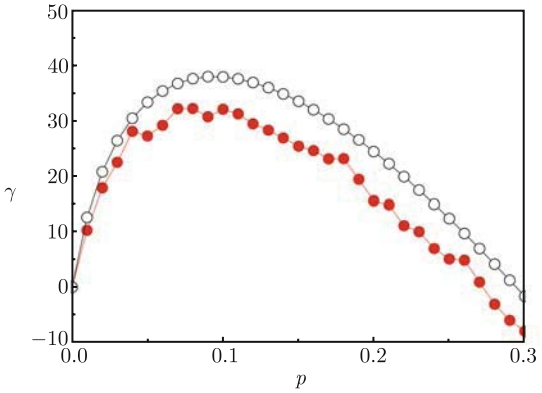

Fig. 12 γ versus p for $\lambda = 0.1$ and $p_0 \approx 0.1$ where the solid points represent the results of numerical simulations and the hollow points the results from Eqs. (64) and (68).

p makes more infected I_2 and less susceptible $N - I_2$, resulting in that the infected agents do not have sufficient neighbors to be infected and thus reduce the reproducing ability.

Another factor that influences the infected number I_2^* in the safe community A_2 is the average degree $\langle k \rangle_2$. $\langle k \rangle_2$ is determined by both the density of agents and the interaction radius r. The density can be reflected by the size L_2 for a fixed N. From Eq. (66) we have

$$\begin{aligned} \frac{I_1^*}{I_2^*} &= \frac{1}{\lambda \langle k \rangle_2 p} - \frac{1-p}{p} \\ &= \frac{L_2^2}{\lambda \pi r^2 N p} - \frac{1-p}{p} \end{aligned} \tag{69}$$

It is easy to see that for a fixed p, I_1^*/I_2^* is inversely proportional to the average degree of the safe community $\langle k \rangle_2$, i.e., proportional to L_2^2 and inversely proportional to r^2. To keep $\lambda = 0.1$ in between $[\lambda_{c1}, \lambda_{c2}]$, we let L_2 increase from 1 to 2.4 for $r = 0.05$ and let r change from 0.03 to 0.055 for $L_2 = 1$. Our numerical simulations have confirmed the prediction Eq. (69), see Fig. 13 for three typical $p = 0.025, 0.05$ and 0.1 where (a) represents the relationship between I_1^*/I_2^* and L_2^2 and (b) I_1^*/I_2^* versus $1/r^2$.

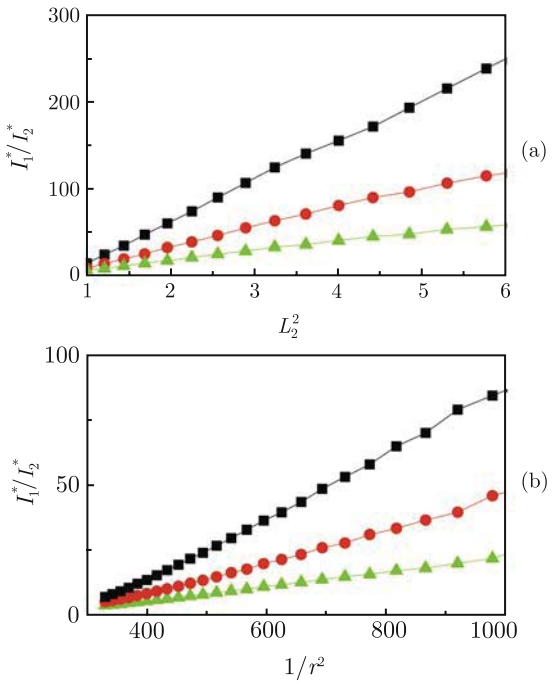

Fig. 13 How the parameters L_2 and r influence the ratio I_1^*/I_2^* for $L_1 = 0.5$ and $\lambda = 0.1$ where the lines with "squares", "circles", and "triangles" denote the cases of $p = 0.025$, 0.05 and 0.1, respectively, and **(a)** represents the relationship between I_1^*/I_2^* and L_2^2 for $r = 0.05$ and **(b)** I_1^*/I_2^* versus $1/r^2$ for $L_2 = 1$.

After understanding the mechanism of epidemic

spreading in a model of two communities, let us move to the model of three communities, i.e., epidemic spreading through an indirect contagion. This situation occurs very often in reality. For example, when an epidemic breaks out in a community, its surrounding communities will usually remove the links with it to keep their safety. While for those communities not connected directly to the infected one, they will not remove the connections to their surroundings. Suppose one neighbor of the infected community does not remove its links between them in time, how the neighbor's neighbor is influenced by the infected community through an indirect way? To solve this problem, let's construct a model of three communities as shown in Fig. 14 where A_1 denotes the infected community with higher density of agents, A_2 and A_3 denote the safe communities with lower density of agents. The jumping is allowed between A_1 and A_2 and also between A_2 and A_3 but forbidden between A_1 and A_3. For simplicity, we let all the three communities have the same population $N = 1000$ and the same jumping possibilities p between A_1 and A_2 and also between A_2 and A_3. We assume $L_1 < L_2 = L_3$. Hence, the density of agents in A_1 is higher than that in A_2 and A_3, and the epidemic threshold λ_{c1} of A_1 is smaller than λ_{c2} of A_2 and A_3. Like the discussed model of two communities, here we let the three communities have the same contagion rate λ and are also interested in the case of $\lambda_{c1} < \lambda \leqslant \lambda_{c2}$. Making the similar analysis, we find that the safety of the third community cannot be guaranteed even if it is not directly connected with the infected community, see the details in Ref. [73].

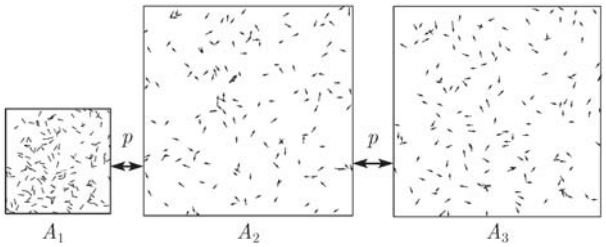

Fig. 14 Schematic illustration of the epidemic spreading in a model of three communities, see text for the detailed explanation.

6 Discussion and envisions

We have briefly reviewed the epidemic and rumor propagation in complex networks, especially in community networks. The main results are as follows: (1) For the rumor propagation in complex networks, we find that the degree distribution influences seriously the final density of infected nodes. The homogeneous networks are more prevalent than the heterogeneous networks. (2) A simplified community model has been presented, which is highly clustered and has nonsymmetric connectivity distribution. We have also constructed a community network model with varying clustering coefficients and varying SF degree distribution to study the influence of community structure on epidemic spreading. This model shows that the clustering is against the epidemic spreading. (3) A dynamical community network is presented to discuss the influence of the mobile feature of agents on the epidemic spreading. We find that for the case of direct and indirect connection, it is possible to sustain an epidemic spreading even when the contagion rate λ is smaller than its critical threshold, which is impossible for an isolated community.

Recently, epidemics in a metapopulation have received a lot of interest [74−79]. In this case, the epidemic spreading is considered as a kind of reaction-diffusion (RD) process. The individuals can move between different locations, such as cities or urban areas. The reaction processes account for the possibility that individuals in the same location may get in contact and change their state according to the infection dynamics, and the diffusion processes account for the spreading of the epidemic. It is found that the diffusion process is a super-diffusion on structured networks.

Models, based on RD, can be used not only in slowing the spread of infectious diseases, but also in chemical reaction, optimizing traffic flow, or predicting the change in cell phone usage in a disaster. Therefore, the methods developed in other related fields may be helpful for the study of epidemic spreading in a metapopulation. Because any model should be confirmed by experiments or real data, a hopeful direction of studying epidemic spreading may be data mining. In that case we may imagine that both the random mixture and network structure are important, and their combined results are closer to the real data.

Acknowledgements This work was partially supported by the National Natural Science Foundation of China (Grant Nos. 10775052 and 10635040), SPS (Grant Nos. 05SG27 and NCET-05-0424), and Program for Changjiang Scholars and Innovative Research Team.

References

1. R. Albert and A.-L. Barabasi, Rev. Mod. Phys., 2002, 74: 47
2. S. Boccaletti, V. Latora, Y. Moreno, M. Chavez, and D.-U. Hwang, Phys. Rep., 2006, 424: 175
3. F. Liljeros, C. R. Edling, L. A. Amaral, H. E. Stanley, and Y. Aberg, Nature, 2001, 411: 907
4. Z. Liu, Y.-C. Lai, and N. Ye, Phys. Rev. E, 2002, 66:

036112
5. Z. Liu, Y.-C. Lai, and N. Ye, Phys. Lett. A, 2002, 303: 337
6. Z. Liu, Y.-C. Lai, and N. Ye, Phys. Rev. E, 2003, 67: 031911
7. H. Zhang, Z. Liu, and W. Ma, Chin. Phys. Lett., 2006, 23: 1050
8. D.-F. Zheng, P. M. Hui, S. Trimper, and B. Zheng, Physica A, 2005, 352: 659
9. G. Yan, T. Zhou, J. Wang, Z.-Q. Fu, and B.-H. Wang, Chin. Phys. Lett., 2005, 22: 510
10. Y. Lu, M. Zhao, T. Zhou, and B.-H. Wang, Phys. Rev. E, 2007, 76: 057103
11. Z. Gu, M. Zhao, T. Zhou, C. Zhu, and B.-H. Wang, Phys. Lett. A, 2007, 362: 115
12. D. Jun and D. He, Chin. Phys. Lett., 2007, 24: 3355
13. H. Chang, B. Su, Y. Zhou, and D. He, Physica A, 2007, 383: 687
14. M. Kuperman and G. Abramson, Phys. Rev. Lett., 2001, 86: 2909
15. M. Barahona and L. M. Pecora, Phys. Rev. Lett., 2002, 89: 054101
16. V. M. Eguiluz and K. Klemm, Phys. Rev. Lett., 2002, 89: 108701
17. M. E. J. Newman, Phys. Rev. Lett., 2002, 89: 208701
18. Z. Liu, W. Ma, H. Zhang, Y. Sun, and P. M. Hui, Physica A, 2006, 370: 843
19. M. Tang, Z. Liu, and J. Zhou, Phys. Rev. E, 2006, 74: 036101
20. H. Zhang, Z. Liu, M. Tang, and P. M. Hui, Phys. Lett. A, 2007, 364: 177
21. Z. Liu and P. M. Hui, Physica A, 2007, 383: 714
22. Z. Liu and B. Li, Phys. Rev. E, 2007, 76: 051118
23. N. M. Ferguson, M. J. Keeling, W. J. Edmunds, R. Gani, B. T. Grenfell, B. M. Anderson, and S. Leach, Nature, 2003, 425: 681
24. D. A. Cummings, R. A. Irizarry, N. E. Huang, T. P. Endy, A. Nisalak, K. Ungchusak, and D. S. Burke, Nature, 2004, 427: 344
25. L. Stone, R. Olinky, and A. Huppert, Nature, 2007, 446: 533
26. N. M. Ferguson, C. A. Donnelly, and B. M. Anderson, Science, 2001, 292: 1155
27. M. E. J. Newman and J. Park, Phys. Rev. E, 2003, 68: 036122
28. M. E. J. Newman and M. Girvan, Phys. Rev. E, 2004, 69: 026113
29. E. M. Jin, M. Girvan, and M. E. J. Newman, Phys. Rev. E, 2001, 64: 046132
30. Z. Liu and B. Hu, Europhys. Lett., 2005, 72: 315
31. R. M. Anderson and R. M. May, Infectious Disease of Humans, Oxford: Oxford University Press, 1992
32. N. T. J. Bailey, The Mathematical Theory of Infectious Diseases, 2nd Ed., Berlin, Heidelberg: Springer Verlag, 1993
33. M. Barthelemy, R. Pastor-Satorras, and A. Vespignani, Phys. Rev. Lett., 2004, 92: 178701
34. R. Huerta and L. S. Tsimring, Phys. Rev. E, 2002, 66: 056115
35. R. Pastor-Satorras and A. Vespignani, Phys. Rev. Lett., 2001, 86: 3200
36. M. Boguna, R. Pastor-Satorras, and A. Vespignani, Phys. Rev. Lett., 2003, 90: 028701
37. R. Olinky and L. Stone, Phys. Rev. E, 2004, 70: 030902
38. M. E. J. Newman, Phys. Rev. E, 2002, 66: 016128
39. Y. Moreno, R. Pastor-Satorras, and A. Vespignani, Euro. phys. J. B, 2002, 26: 521
40. Y. Moreno, J. B. Gomez, and A. F. Pacheco, Phys. Rev. E, 2003, 68: 035103
41. Y. Moreno, M. Nekovee, and A. Vespignani, Phys. Rev. E, 2004, 69: 055101
42. H. Zhang, Z. Liu, and W. Ma, Chin. Phys. Lett., 2006, 23: 1050
43. P. Crepey, F. P. Alvarez, and M. Barthelemy, Phys. Rev. E, 2006, 73: 046131
44. A. Vazquez, Phys. Rev. Lett., 2006, 96: 038702
45. T. Zhou, J. Liu, W. Bai, G. Chen, and B. Wang, Phys. Rev. E, 2006, 74: 056109
46. G. Yan, Z. Fu, J. Ren, and W. Wang, Phys. Rev. E, 2007, 75: 016108
47. A. Grabowski and R. A. Kosinski, Phys. Rev. E, 2004, 70: 031908
48. V. Colizza, A. Barrat, M. Barthelemy, and A. Vespignani, Inter. J. Bif. Chaos, 2007, 17: 2491
49. R. Pastor-Satorras and A. Vespignani, Phys. Rev. E, 2001, 63: 066117
50. R. Pastor-Satorras and A. Vespignani, in: Handbook of Graphs and Networks: From the Genome to the Internet, edited by S. Bornholdt and H. G. Schuster, Berlin: Wiley-VCH, 2002: 113
51. A. Sudbury, J. Appl. Prob., 1985, 22: 443
52. D. H. Zanette, Phys. Rev. E, 2001, 64: 050901
53. D. H. Zanette, Phys. Rev. E, 2002, 65: 041908
54. Y. Moreno, M. Nekovee, and A. F. Pacheco, Phys. Rev. E, 2004, 69: 066130
55. J. Zhou, Z. Liu, and B. Li, Phys. Lett. A, 2007, 368: 458
56. P. Holme and B. J. Kim, Phys. Rev. E, 2002, 65: 026107
57. J. Noh, H. Jeong, Y. Ahn, and H. Jeong, Phys. Rev. E, 2002, 71: 036131
58. J. Sun and M. W. Deem, Phys. Rev. Lett., 2007, 99: 228107
59. J. M. Kumpula, J. Onnela, J. Saramaki, K. Kaski, and J. Kertesz, Phys. Rev. Lett., 2007, 99: 228701
60. X. Wu and Z. Liu, Physica A, 2008, 387: 623
61. J. Marro and R. Dickman, Nonequilibrium Phase Transitions in Lattice Models, Cambridge: Cambridge University Press, 1999
62. Y. Zhou, Z. Liu, and J. Zhou, Chin. Phys. Lett., 2007, 24: 581
63. A. Vecchio, L. Primavera, and V. Carbone, Phys. Rev. E, 2006, 73: 031913
64. D. H. Zanette and M. Kuperman, Physica A, 2002, 309: 445

65. R. Cohen, S. Havlin, and D. Ben-Avraham, Phys. Rev. Lett., 2003, 91: 247901
66. R. Pastor-Satorras and A. Vespignani, Phys. Rev. E, 2002, 65: 036104
67. L. K. Gallos, F. Liljeros, P. Argyrakis, A. Bunde, and S. Havlin, Phys. Rev. E, 2007, 75: 045104
68. T. Vicsek, A. Czirok, E. Ben-Jacob, I. Cohen, and O. Shochet, Phys. Rev. Lett., 1995, 75: 1226
69. A. Buscarino, L. Fortuna, M. Frasca, and A. Rizzo, Chaos, 2006, 16: 015116
70. M. Gonzalez and H. J. Herrmann, Physica A, 2004, 340: 741
71. M. Frasca, A. Buscarino, A. Rizzo, L. Fortuna, and S. Boccaletti, Phys. Rev. E, 2006, 74: 036110
72. M. Gonzalez, P. G. Lind, and H. J. Herrmann, Phys. Rev. Lett., 2006, 96: 088702
73. J. Zhou and Z. Liu, Epidemic Spreading in Dynamical Community Networks, unpublished
74. V. Colizza, R. Pastor-Satorras, and A. Vespignani, Nature Phys., 2007, 3: 276
75. V. Colizza and A. Vespignani, Phys. Rev. Lett., 2007, 99: 148701
76. S. Riley, Science, 2007, 316: 1298
77. G. Chowell, J. M. Hyman, S. Eubank, and C. Castillo-Chavez, Phys. Rev. E, 2003, 68: 066102
78. S. Eubank, H. Guclu, V. S. Anil Kumar, M. V. Marathe, A. Srinivasan, Z. Toroczkai, and N. Wang, Nature, 2004, 429: 180
79. E. Agliari, R. Burioni, D. Cassi, and F. M. Neri, Phys. Rev. E, 2006, 73: 046138